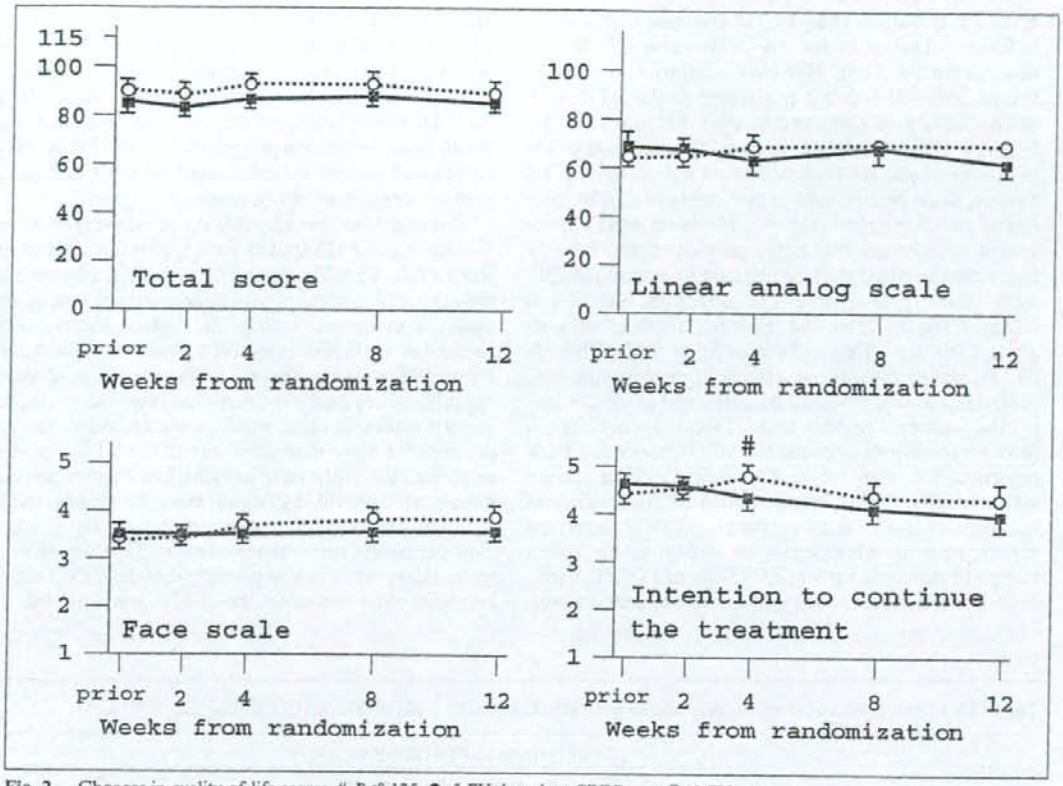

Fig. 2 - Changes in quality-of-life scores. #, P<0.125. ●, 5-FU+low-dose CDDP arm. ○, 5-FU arm.

14). An ideal chemotherapy would provide long survival without severe toxicities or deterioration of QOL.

Three phase III clinical trials comparing continuous infusion of 5-FU versus continuous infusion of 5-FU+low-dose CDDP for CRC are reported in literature (2, 15, 16). In these previous studies, all conducted in the United States, response rates were similar or significantly higher in the 5-FU+CDDP treatment groups than in the 5-FU treatment groups. However, increased toxicity and no improvement in OS were observed in the 5-FU+CDDP treatment group (Tab. V). The dose of CDDP was 20 mg/m²/day one to five times a week in the previous US trials for CRC, while substantially lower doses (3.5-7.5 mg/m²/day for five consecutive days per week) were given in the treatment of gastric cancer in Japan (4-6). The JFMC performed the low-dose (1-6 mg/m²/day) and consecutive administration (five times a week) of CDDP with novel oral fluoropyrimidine S-1 for gastric cancer as a phase I trial, and observed an acceptable level of toxicity as well as a promising degree of efficacy (17). It is interesting that patients with CRC may receive a survival benefit and strong efficacy from a similar very low-dose and frequent administration of CDDP with continuous infusion of 5-FU. In this study, CDDP was given at a dose of 3 mg/m² on days 1-5 and 8-12. Five weekly administrations of CDDP are difficult to manage on an outpatient basis. To shorten hospitalization, CDDP was given at a dose of 7 mg/m² twice a week at 2- or 3-day intervals in the third week and later. The CDDP dosages in this study were determined on the basis of a previous report; it was demonstrated that the CDDP administration of 7 mg/m² twice a week maintained the serum CDDP concentration which was attained by the 5 time administrations of 3.5 mg/m² CDDP per week (18).

The backgrounds of the two arms were well bal-

anced in this study (Tab. I). The response rate was significantly higher in the 5-FU+low-dose CDDP arm than in the 5-FU arm. However, contrary to our expectation, survival was not prolonged in the 5-FU+low-dose CDDP arm compared to the 5-FU arm (Tab. III, Fig. 1). These results are consistent with those of the previous phase III studies carried out in the United States; those studies used higher doses of CDDP compared to our regimen (Tab. V). However, MSTs in our series were longer than in the previous trials (Tab. V). Improved survival may be attained by a multidisciplinary therapy including the effective second-line chemotherapies after the 12-week regimen in both arms (Tab. II). Although the addition of CDDP to 5-FU enhanced the adverse effects of neutropenia, anemia, and nausea, it should be noted that grade 3/4 toxicities were rare in both arms (Tab. VI). Therefore, it may be feasible to continue the 5-FU+low-dose CDDP regimen for more than 12 weeks without severe adverse effects. The low toxicities of the continuous infusion of 5-FU with or without CDDP described above were an advantage with respect to the recent standard regimens such as FOLFOX or FOLFILI with or without bevacizumab, a molecular targeting agent. However, the necessity for the patient to carry a balloon pump for most of the treatment period of twelve weeks and to come to hospital for CDDP infusion twice a week may be a disadvantage.For example, in the "FOLFOX6" regimen, the patient is restrained only for 46 hrs with balloon pump infusion of 5-FU and visits hospital at day 1 for infusion of 5-FU/LV and oxaliplatin every course of two weeks.

It was also noteworthy that the response rates of the 5-FU arm in the US studies were higher than that in our study (Tab. V). This difference may be attributable to the evaluation method, particularly with regard to the observation period; in the US studies, the response rates were evaluated every 8-12 weeks until the tumor showed PD or the patient died, whereas in the 12-week regimen of our study the response rate was evaluated every 4 weeks. In other words, if we had continued the regimen for more than 12 weeks in the 5-FU arm, the response rate might have been higher. Further prolongation of survival by more than 12 weeks in 5-FU+low-dose CDDP might also be expected when considering the survival achieved by the 12-week regimen. However, it is also possible that the difference of response rates between the 5-FU arm and the 5-

Table IV - Comparison of chemotherapeutic adverse effects between 5-FU+low-dose CDDP arm and 5-FU arm

Features	% of Patients (5-FU+CDDP vs 5-FU)				*P* value
	Grade 1	Grade 2	Grade 3	Grade 4	
Hematologic					
Neutropenia	16.2 vs 11.8	18.9 vs 3.9	8.1 vs 0	0 vs 0	<.001
Thrombocytopenia	2.7 vs 1.3	2.7 vs 1.3	0 vs 1.3	1.4 vs 0	0.497
Anemia	12.2 vs 13.2	16.2 vs 9.2	6.8 vs 0	0 vs 0	0.015
Nonhematologic					
Nausea	28.4 vs 7.9	6.8 vs 3.9	4.1 vs 2.6	NA	0.012
Vomiting	6.8 vs 6.6	5.4 vs 1.3	0 vs 1.3	0 vs 1.3	0.928
Diarrhea	2.7 vs 3.9	1.4 vs 2.6	1.4 vs 2.6	0 vs 0	0.374
Stomatitis	10.8 vs 11.8	1.4 vs 1.3	0 vs 0	0 vs 0	0.879
Hand-foot syndrome	13.5 vs 7.9	1.4 vs 3.9	0 vs 0	NA	0.952
Eruption/Exfoliation	2.7 vs 1.3	4.1 vs 1.3	0 vs 0	0 vs 0	0.229
Alopecia	2.7 vs 1.3	0 vs 0	NA	NA	0.556
Fatigue	10.8 vs 6.6	8.1 vs 2.6	2.7 vs 2.6	0 vs 1.3	0.407
Arrhythmia	1.4 vs 1.3	0 vs 0	0 vs 0	0 vs 0	0.985
Albumin	16.2 vs 10.5	5.4 vs 2.6	1.4 vs 1.3	0 vs 0	0.241
Total bilirubin	10.8 vs 9.2	4.1 vs 2.6	4.1 vs 0	0 vs 1.3	0.305
AST	16.2 vs 23.7	5.4 vs 2.6	1.4 vs 0	0 vs 1.3	0.768
ALT	6.8 vs 14.5	1.4 vs 1.3	1.4 vs 2.6	0 vs 0	0.203
Creatinine	14.9 vs 5.3	0 vs 3.9	0 vs 0	0 vs 0	0.795

5-FU, 5-fluorouracil. CDDP, cisplatin. NA, not applicable.
Numbers of patients in 5-FU+low-dose CDDP group and 5-FU group were 74 and 76, respectively.

Table V - Randomized trials comparing continuous infusional 5-fluorouracil with or without cisplatin

References	Dose	Response rate			MST (Months)		
		5-FU+CDDP	5-FU	*P*-value	5-FU+CDDP	5-FU	*P*-value
Kemeny (1990)	5-FU 1000 mg/m² days 1 to 5 CDDP 20 mg/m² days 1 to 5 repeat every 4 weeks	25% (15/61)	3% (2/59)	0.001	10	12	NS
Lokich (1991)	5-FU 300 mg/m² every day CDDP 20 mg/m²	33% (25/85) weekly	35% (29/83)	NS	11.2	11.8	NS
Hansen (1996)	5-FU 300 mg/m² every day CDDP 20 mg/m² weekly	31% (47/153)	28% (45/159)	NS	13	13	NS
Present study	5-FU 300 mg/m² days 1 to 5 repeat every week CDDP 3 mg/m² days 1 to 5, 8 to 12 followed by 7 mg/m² twice a week for 10 weeks	25.3% (20/75)	11.7% (9/77)	0.037	15.7	16.1	NS

5-FU, 5-fluorouracil. CDDP, cisplatin. MST, median survival time; NS, not significant.

FU+low-dose CDDP arm in this 12-week regimen might be lost during the longer treatment period than 12 weeks. These speculations should be tested by a further clinical trial.

Recently, the QOL in patients following a chemotherapy regimen has attracted much attention and has been evaluated in clinical trials (11, 12). In the present study, QOL questionnaires answered by the patients themselves were analyzed, whereas the three previous phase III trials of 5-FU+low-dose CDDP for CRC did not use self-reporting questionnaires (2, 15, 16). No statistically significant differences between the arms were found, except for the intention to continue treatment at 4 weeks from randomization. This may mean that the addition of CDDP to 5-FU administration scarcely deteriorated the QOL during the 12-week regimen (Fig. 2).

Taken together, the results indicate that 5-FU+low-dose CDDP for CRC may be given safely and attain moderate tumor reduction. However, this combination chemotherapy did not improve survival and induced slightly higher adverse events, compared to continuous infusion of 5-FU. Taking into account the additional cost of CDDP infusion twice a week, the 5-FU+low-dose CDDP in the short regimen setting of 12 weeks rendered no clinical benefit.

Acknowledgments. We wish to thank a number of physicians and their institutions that are not listed among the article's co-authors, including physicians at Sapporo Medical University School of Medicine, Juntendo University Urayasu Hospital, Osaka Medical Center for Cancer and Cardiovascular Diseases, NTT West Osaka Hospital, Wakayama Medical University,

Kumamoto Rosai Hospital, Iwate Medical University School of Medicine, Yokoyama Gastroenterological Hospital, Kansai Rosai Hospital, University of Yamanashi, Nagoya Medical Center, Izumi City Hospital, Osaka Ekisaikai Hospital, Tottori Municipal Hospital, and Kumamoto Municipal Hospital. We are also thankful to T. Takeuchi, Y. Kawamura, and M. Nakashima of JFMC for their assistance in data collection. We appreciate the extramural reviewers' dedication to the evaluation of patient eligibility and response to treatment: K. Kumai and N. Tanimoto, Keio University; M. Kusano, Showa University; and T. Sekine, Hasuda Hospital. We are also grateful to the following surgical oncologists and specialists in statistics for their academic assistance: S. Saji, JFMC; J. Sakamoto, Kyoto University; M. Nishiyama, Hiroshima University; and Y. Ohashi, Tokyo University.

References

1. Lokich J.J., Ahlgren J.D., Gullo J.J., et al: A prospective randomized comparison of continuous infusion fluorouracil with a conventional bolus schedule in metastatic colorectal carcinoma: a Mid-Atlantic Oncology Program Study. J. Clin. Oncol. 7:425-432, 1989.
2. Hansen R.M., Ryan L., Anderson T., et al: Phase III study of bolus versus infusion fluorouracil with or without cisplatin in advanced colorectal cancer. J. Natl. Cancer Inst. 88:668-674, 1996.
3. The Meta-analysis Group in Cancer: Efficacy of intravenous continuous infusion of fluorouracil compared with bolus administration in advanced colorectal cancer. J. Clin. Oncol. 16:301-308, 1998.
4. Kondo K., Murase M., Kodera Y., et al: Feasibility study on protracted infusional 5-fluorouracil and consecutive low-dose cisplatin for advanced gastric cancer. Oncology 53:64-67, 1996.
5. Chung Y.S., Yamashita Y., Inoue T., et al: Continuous infusion of 5-fluorouracil and low dose cisplatin infusion for the treatment of advanced and recurrent gastric adenocarcinoma. Cancer 80:1-7, 1997.
6. Kim R., Murakami S., Ohi Y., et al: A phase II trial of low dose administration of 5-fluorouracil and cisplatin in patients with advanced and recurrent gastric cancer. Int. J. Oncol. 15:921-926, 1999.
7. Scanlon K.J., Newman E.M., Lu Y., et al: Biochemical basis for cisplatin and 5-fluorouracil synergism in human ovarian carcinoma cells. P. Natl. Acad. Sci. USA 83:8923-8925, 1986.
8. Shirasaka T., Shimamoto Y., Ohshimo H., et al: Metabolic basis of the synergistic antitumor activities of 5-fluorouracil and cisplatin in rodent tumor models in vivo. Cancer Chemoth. Pharm. 32:167-172, 1993.
9. Araki H., Fukushima M., Kamiyama Y., et al: Effect of consecutive lower-dose cisplatin in enhancement of 5-fluorouracil cytotoxicity in experimental tumor cells in vivo. Cancer Lett. 160:185-191, 2000.
10. Kurihara M., Shimizu H., Tsuboi K., et al: Development of quality of life questionnaire in Japan: quality of life assessment of cancer patients receiving chemotherapy. Psycho-Oncol. 8:355-363, 1999.
11. de Gramont A., Figer A., Seymour M., et al: Leucovorin and fluorouracil with or without oxaliplatin as first-line treatment in advanced colorectal cancer. J. Clin. Oncol. 18:2938-2947, 2000.
12. Saltz L.B., Cox J.V., Blanke C., et al: Irinotecan plus fluorouracil and leucovorin for metastatic colorectal cancer. Irinotecan Study Group. New Engl. J. Med. 343:905-914, 2000.
13. Tournigand C., Andre T., Achille E., et al: FOLFIRI followed by FOLFOX6 or the reverse sequence in advanced colorectal cancer: a randomized GERCOR study. J. Clin. Oncol. 22:229-237, 2004.
14. Rothenberg M.L., Meropol N.J., Poplin E.A., et al: Mortality associated with irinotecan plus bolus fluorouracil/leucovorin: summary findings of an independent panel. J. Clin. Oncol. 19:3801-3807, 2001.
15. Kemeny N., Israel K., Niedzwiecki D., et al: Randomized study of continuous infusion fluorouracil versus fluorouracil plus cisplatin in patients with metastatic colorectal cancer. J. Clin. Oncol. 8:313-318, 1990.
16. Lokich J.J., Ahlgren J.D., Cantrell J., et al: A prospective randomized comparison of protracted infusional 5-fluorouracil with or without weekly bolus cisplatin in metastatic colorectal carcinoma. A Mid-Atlantic Oncology Program study. Cancer 67:14-19, 1991.
17. Nakata B., Mitachi Y., Tsuji A., et al: Combination phase I trial of a novel oral fluorouracil derivative S-1 with low-dose cisplatin for unresectable and recurrent gastric cancer (JFMC-27-9902). Clin. Cancer Res. 10:1664-1669, 2004.
18. Yagihashi A., Sasaki K., Hirata K., et al.: Study of serum CDDP concentrations in patients with advanced or recurrent adeno-or squamous cell carcinoma under combination chemotherapy of 5-FU (CIV) and low-dose CDDP (IV). Gan to Kagaku Ryoho (Jpn. J. Cancer Chemother.) 23:63-67, 1996.

Received: July 7, 2006

Bunzo Nakata, M.D.,
Department of Surgical Oncology,
Osaka City University Graduate School of Medicine,
1-4-3 Asahimachi, Abeno-ku, Osaka 545-8585, Japan.
Phone: +81-6-6645-3838
Fax: +81-6-6646-6450
E-mail: bunzo@med.osaka-cu.ac.jp

外来がん化学療法と地域連携

近年，対象患者数の増加や diagnosis procedure combination（DPC）をはじめとする医療状況の変化により，がん化学療法は入院から外来への移行が進んでいる。また一方でがん連携拠点病院の指定などにより，がん化学療法患者の拠点病院への一極集中が強まりつつある。このため，都市圏では増加の一途をたどる患者数に対応するため，また地域では医療資源の不足に対応するために，地域連携は，がん化学療法における重要事項となり，地域医療機関も積極的に受け入れの準備を進めるようになった。

ところが実際の地域連携は思いのほか進んでおらず，このことは多くの拠点病院共通の問題点ともなっている。なぜこういったことが起こっているのだろうか。実際には，地域の病院は，可能な患者は受け入れたいと考えている。それなのになぜ受け入れがうまくいっていないのだろうか。この問題に関しては化学療法のハードルが高いからなどといった声もよく聞かれる。ではハードルが高くなっている原因はなんであろうか。“担当医の個人的関係での連携”の限界や“地域連携室相互のコミュニケーション経験不足”などが理由にあげられているが，実際にはさらに基本的なところに問題点があるように感じられる。

現在の地域連携では，いわゆる“手間のかかる患者さん”の層が多くを占めている一方で，good risk で収益が上がり，“手間のかからない患者さん”は地域連携の対象患者となることは少なく，主治医はそういった患者は連携を行わず手元に置きがちであった。つまり“ハードルが高い患者さん”を連携の主な対象としていたために，連携が進んでこなかったのではないだろうか。

実際，高知医療センターにおける初期の連携時には，種々の理由により連携先に根付かない患者もみられた。しかし連携対象患者のセレクションを行い，“手のかかる患者さんは紹介を延期し，副作用の十分なマネージメントを行ったのち，状況が良くなった患者さんから紹介する”を基本方針として以降は，連携先とのこういった問題点は解消した。「自分がやって楽勝」と思うようでないとなかなか他所ではやってもらえないし，さらには「こんなに楽でいいのかな」と簡単に実績が上げられることを連携先に知ってもらうことで，従来障害となっていたハードルを取り去ることが可能ではないかと思われる。こういったことは従来，拠点病院の担当医が紹介先である連携病院の担当医に「もう少し状況の良い人を紹介してほしい」「もう少し早くに紹介してほしい」と感じていたことと，表裏をなしているのではないだろうか。

地域連携は患者のためのものであり，患者主体の地域連携のために，成熟した連携システムの構築が必須である。連携の担当者はこれらのことを十分に理解したうえで地域連携を開始することが重要である。野球のキャッチボールも，上手な人が教えるときには，取りやすくやさしい球から始め，しだいに速い球を投げるように，地域連携も連携しやすい患者から始め，経験を積み重ねれば，しだいにリスクの高い患者の連携も可能となってくるのではないかと思われる。化学療法に習熟した担当医が連携を指導すれば，早く上手になり，レベルの高い地域連携ができるのは自明の理である。そして“手間のかからない患者さん”でも数多く連携を行うことで，拠点病院の診療は実際楽

になっていくし，連携先は収益も向上し，さらなる受け入れを行ってくれるだけでなく，長期的には紹介患者の増加にもつながるなど，メリットも多いと思われる（図1）。

また一方で，十分な患者教育を行い患者のレベルアップ向上を行うことや，化学療法のマニュアル化などによる拠点病院連携先医療機関のレベルアップや医療情報，ノウハウの共有など必須である（当院では『がん化学療法施行時の検査，有害事象対策の手引き』を作成し，地域へも配布している）。こういったことにより“手間のかからない患者さん”を増加させ，さらに連携が広がっていくことが期待される。

また，連携先医療機関のレベルアップに努め，地域での標準治療の確実な施行を可能とするがん治療の均てん化を推進することで，患者のがん化学療法に対する意識も変わり，「近くにコンビニがあるのにわざわざ遠くのコンビニまで買い物に行くことはない」のと同じように，「標準的化学療法を行うのに，わざわざ遠方のがん拠点病院に毎回受診する必要はない」となってくることが期待される。

いずれにせよ，今後は拠点病院ばかりでなく，地域の医療機関にとってもがん化学療法の地域連携は最重要事項のひとつとなってくると思われる。地域連携室などの整備も進みつつあるが，まずは確実に連携できそうな患者を担当医と連携担当者で選定し，経験を深め，地域連携の基盤構築を進めるべきではないかと感じている。さらには患者，地域および拠点病院の三位一体のレベルアップを行っていくことにより，がん化学療法の地域連携は成熟していくのではないだろうか。

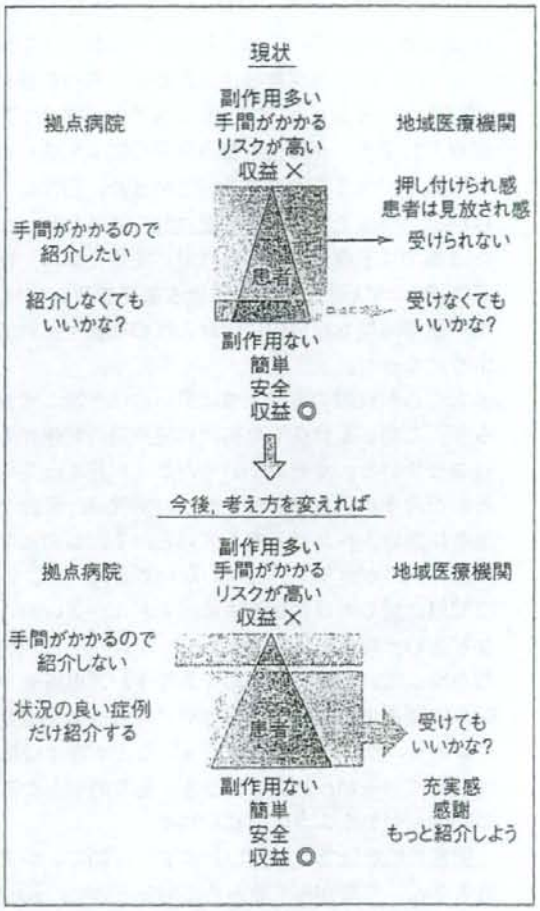

図 1　がん化学療法における地域連携

辻　晃仁
（高知医療センター　腫瘍内科 旧化学療法科）

CDC25A inhibition suppresses the growth and invasion of human hepatocellular carcinoma cells

XUNDI XU[1,2], HIROFUMI YAMAMOTO[1], GUOXING LIU[2], YASUHIRO ITO[1], CHEW YEE NGAN[1], MOTOI KONDO[1], HIROAKI NAGANO[1], KEIZO DONO[1], MITSUGU SEKIMOTO[1] and MORITO MONDEN[1]

[1]Department of Surgery, Gastroenterological Surgery, Graduate School of Medicine, Osaka University, Osaka 565-0871, Japan; [2]Department of Surgery, Xiangya Second Hospital, Central South University, Changsha, Hunan province 410011, P.R. China

Received May 31, 2007; Accepted July 9, 2007

Abstract. CDC25A is a cell cycle-activating phosphatase that promotes transition from the G1 to S phase. We previously reported that overexpression of CDC25A in human hepatocellular carcinoma (HCC) tissue samples was associated with poor prognosis. In this study, we attempted suppression of CDC25A in HCC cells to elucidate the therapeutic potential of this approach. Administration of CDC25A antisense (AS) oligonucleotide resulted in 25-50% inhibition of cell growth at 48 h, G0-G1 arrest, and significant inhibition of cancer cell invasion. To elucidate the underlying mechanism of the inhibitory effects of HCC cell invasion, we examined several invasion-associated molecules, and we found that membrane-type 3 (MT3)-matrix metalloproteinase (MMP) mRNA was greatly reduced following treatment with AS oligonucleotide to CDC25A or siRNA treatment. Notably, screening of a panel of gastrointestinal cancer cells indicated that MT3-MMP was generally expressed by HCC cells, whereas other cell types did not express this type of matrix metalloproteinase so frequently. We also found that CDC25A facilitated cellular differentiation by increasing albumin expression in the PLC cell line. These results suggest that CDC25A, by inhibiting HCC growth and invasion, may be a feasible therapeutic target for human HCC.

Correspondence to: Dr Hirofumi Yamamoto, Department of Surgery, Gastroenterological Surgery, Graduate School of Medicine, Osaka University, 2-2 Yamada-oka, Suita-City, Osaka 565-0871, Japan
E-mail: kobunyam@surg2.med.osaka-u.ac.jp

Abbreviations: AS, antisense; CDK, cyclin-dependent kinase; dsRNAs, double-stranded RNAs; HCC, hepatocellular carcinoma; MMP, matrix metalloproteinase; MM, mismatch; PBGD, porphobilinogen deaminase; PCNA, proliferating cell nuclear antigen; RT-PCR, reverse transcriptase-polymerase chain reaction; siRNA, short interfering RNA

Key words: CDC25A, membrane-type 3-matrix metalloproteinase, hepatocellular carcinoma, invasion, differentiation

Introduction

Primary hepatocellular carcinoma (HCC) is the third leading cause of cancer death worldwide, with an estimated 564,000 new cases in 2000 (1). Frequent postoperative recurrence of the disease, characterized by intrahepatic metastasis or multicentric carcinogenesis, is one of the major reasons for the poor prognosis of HCC (2,3). Insight into the molecular mechanisms involved in hepatocarcinogenesis may enable more effective treatment for HCC.

CDC25 genes are cell cycle-activating phosphatases that remove the inhibitory phosphates of threonine and tyrosine residues at the ATP-binding sites of cyclin-dependent kinase. Three CDC25 genes, CDC25A, CDC25B, and CDC25C, which share ~40-50% amino acid identity, have been identified and function during different stages of the cell cycle, including G1-S and G2-M transition (4-7). It has been found that CDC25A and CDC25B, but not CDC25C, possess oncogenic potential and are able to transform primary murine fibroblasts in cooperation with either mutated Ha-ras or loss of Rb1 (8). Furthermore, concordant *in vitro* and *in vivo* findings show that CDC25A and CDC25B are overexpressed in various types of human malignancies, including HCC (9-14).

Accumulating evidence suggests that several molecules acting at the G1-S transition of the cell cycle play crucial roles in the progression of HCC. HCC tissues overexpress cyclins D1 and E (15,16). In a subset of HCCs, expression of the cyclin-dependent kinase (CDK) inhibitor $p21^{waf1/cip1}$ was reduced, the $p16^{INK4}$ gene was methylated at the promoter region, and expression of $p27^{Kip1}$ appeared to be decreased (15,17,18). We previously found that CDC25A, rather than CDC25B, was overexpressed in the dedifferentiated phenotype of HCC and that its levels correlated with hypergrowth activity (14). We also found that CDC25A overexpression was associated with shorter disease-free survival of patients with HCC. Foundational research showed that ablation of CDC25A function by microinjection of a specific antibody blocks cell entry into S phase (5). Conversely, inducible overexpression of CDC25A, leading to activation of cyclin E-Cdk2 and cyclin A-Cdk2, revealed that these complexes act as critical targets for CDC25A (19,20). This evidence suggests the relevance of CDC25A to G1-S transition. Based

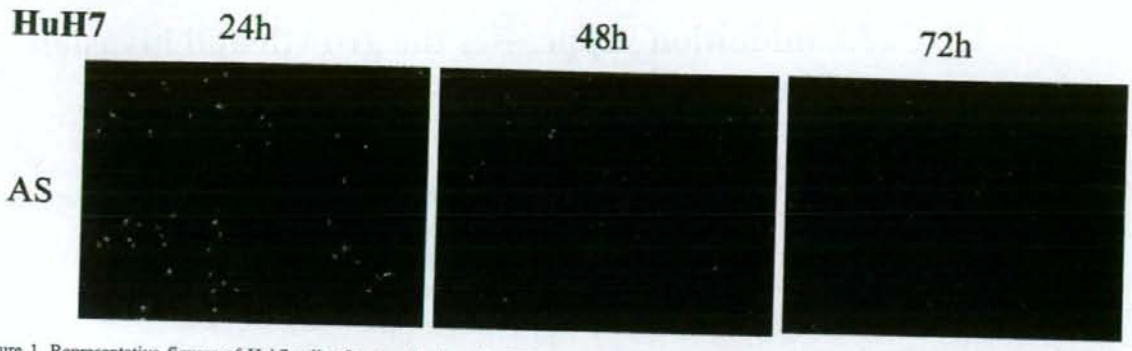

Figure 1. Representative figures of Huh7 cells after transfection with FITC-conjugated antisense (AS) oligonucleotides. Cell count indicated transfection efficiency at 84.1, 88.0 and 89.7% at 24, 48 and 72 h, respectively.

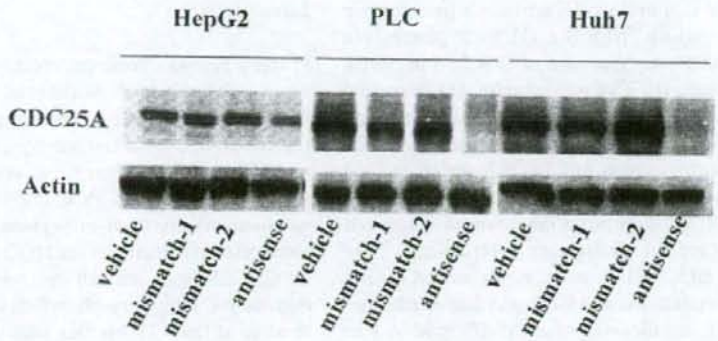

Figure 2. AS oligonucleotide to CDC25A decreased CDC25A expression in HCC cells. Three HCC cell lines were transfected with vehicle alone, vehicle plus MM oligonucleotides, or AS oligonucleotides. Cells were harvested 48 h after transfection. The protein lysates were subjected to Western blot analysis with anti-CDC25A and anti-actin antibody. Actin bands indicate equal loading of the protein.

MT2-MMP reverse, 5'-CTT TCA CTC GTA CCC CGA AC-3'; MT3-MMP forward, 5'-ACA GTC TGC GGA ACG GAG CAG-3' and MT3-MMP reverse, 5'-GTC AAT TGT GTT TCT GTC CAC-3'.

Statistical analysis. Data were expressed as the mean ± SEM. Group differences were examined for statistical significance using the Mann-Whitney U test or Fisher's exact test. Mean values were compared using the Student's t-test. A $p<0.05$ denoted a statistically significant difference.

Results

Transfection efficiency. Representative figures of cells transfected with FITC-conjugated oligonucleotides are shown in Fig. 1. PLC cells had a lowest transfection efficiency, with an average of 18.8±4.57 and 19.5±5.76% for AS and MM2, respectively. A tendency of reduction of efficiency with time was noted. A lower efficiency was found for MM1 at 13.2±0.23%. A slightly higher efficiency was noted in HepG2; 29.6±4.20% for AS, 30.3±1.08% for MM2 and similarly a lower rate of 21.9±7.47% for MM1. Reduction of efficiency with time was only observed for MM1. The highest transfection efficiency was observed for Huh7; 87.2±2.79%, 87.5±1.23% and 86.7±5.48 for AS, MM1 and MM2 respectively.

Suppression of CDC25A with antisense oligonucleotides. We used Western blotting to examine the expression of CDC25A protein in HepG2, PLC, and Huh7 HCC cell lines treated with vehicle alone or vehicle plus each oligonucleotide (AS, MM-1, or MM-2) 48 h after transfection. As shown in Fig. 2, the AS oligonucleotide suppressed CDC25A levels by 60% in HepG2 cells and by ~95% in PLC and Huh7 cells. On the other hand, when we examined CDC25B expression no reduction was obtained by AS-CDC25A (data not shown).

Cell growth and cell cycle. AS to CDC25A significantly inhibited cell growth of HepG2, PLC, and Huh7 cells. Statistical significance between cultures treated with AS oligonucleotide versus other oligonucleotides is shown in Fig. 3A. We then performed flow cytometric analysis 24 h after transfection. In the three HCC cell types tested, treatment with AS oligonucleotide increased the G0-G1 phase fraction and decreased the S phase fraction when compared to vehicle-treated cultures. Repeat experiments of cell growth and cell cycle analyses gave similar results. A representative result is shown in Fig. 3B with the following fraction values for

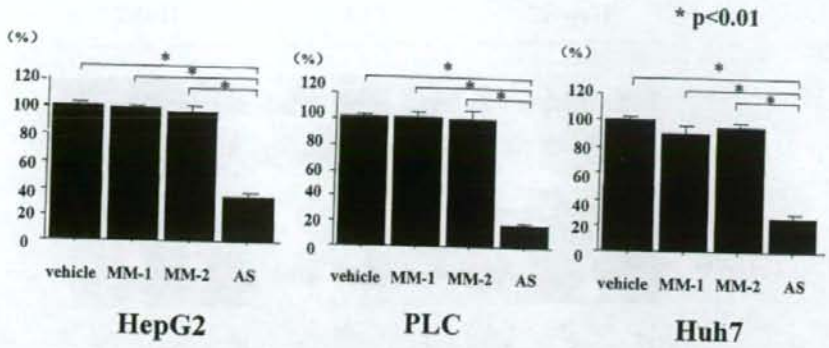

Figure 4. Invasion assay. AS to CDC25A decreased invasion by HCC cells. The assay was performed in duplicate; bars indicate the mean ± SD. A significant reduction in cell invasion was noted in AS-treated cultures versus cultures treated with vehicle, MM-1, and MM-2 (*p<0.01).

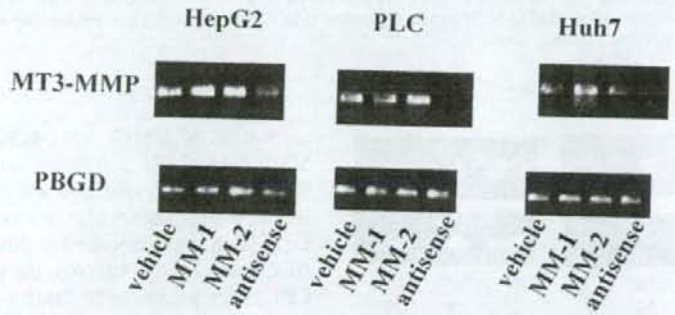

Figure 5. AS to CDC25A decreased MT3-MMP mRNA expression in HCC cells. Cells were harvested 24 h after transfection and examined for MT3-MMP mRNA by RT-PCR assay. PBGD, a housekeeping gene, served as the control. HCC tissues were used as positive control for MT3-MMP mRNA.

Invasive ability. To investigate the effect of AS to CDC25A on the invasive ability of HCC cells we performed an invasive assay. When compared to vehicle treatment, AS to CDC25A significantly suppressed cancer cell invasion by 33.2% in HepG2 cells (p=0.002), 17.2% in PLC cells (p=0.001), and 26.5% in Huh7 cells (p=0.001) (Fig. 4). These inhibitory effects were not found with MM-1 or MM-2 treatment. A repeat experiment showed similar results.

Expression of matrix metalloproteinases. To investigate the underlying mechanism for the inhibitory effect of AS to CDC25A on the invasive ability of HCC cells, we used RT-PCR to examine the expression of a series of matrix metalloproteinases (MMP). These included MMP2, MT1-MMP, MT2-MMP, and MT3-MMP. We found that AS to CDC25A decreased MT3-MMP mRNA expression in all three HCC cell lines (Fig. 5). However, expression of the other MMPs was unaffected (data not shown). To confirm the results, we investigated the effect of siRNA against CDC25A. Western blot analysis showed that the reduction in CDC25A expression was associated with a large reduction in MT3-MMP protein in the three HCC cell lines (Fig. 6).

We then investigated mRNA expression of MMP2, MT1-MMP, MT2-MMP, and MT3-MMP in a variety of gastrointestinal tumor cell lines including HCC cell lines. MT3-MMP expression, when compared to that of other MMPs, was relatively specific to the HCC cell lines (expression rate by cell lines, 7/7:100%) versus other gastrointestinal tumor cell lines such as pancreatic cancer (2/5:40%), colon cancer (0/5: 0%), gastric cancer (1/5:20%), and esophageal cancer (1/3:33%) cell lines (Table 1).

Restoration of albumin expression in PLC by CDC25A inhibition. We investigated whether inhibition of CDC25A restores cell differentiation in HCC cell lines, using albumin expression as a marker of differentiation (24). We found that the PLC cell line which marginally expressed albumin showed an increase in albumin mRNA expression following treatment with AS oligonucleotide (Fig. 7). siRNA treatment against CDC25A showed a similar result (Fig. 7). However, there was no change in albumin mRNA expression in the remaining two HCC cell lines that had relatively high albumin levels (data not shown). We should also emphasize that this was not the case with other liver-specific functions such as APOCIII or asialoglycoprotein receptor, and glutathione-S-transferase-π (data not shown).

Discussion

In our earlier study of CDC25A expression in human HCC tissue samples we found that high CDC25A expression was associated with cell proliferation, portal vein invasion, and

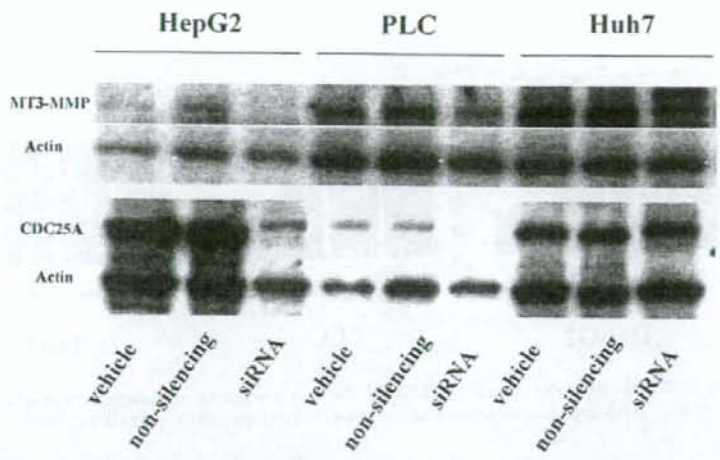

Figure 6. MT3-MMP protein expression was suppressed by siRNA against CDC25A. Cells were collected 48 h after transfection. Inhibition of CDC25A expression by siRNA caused downregulation of MT3-MMP protein expression in HCC cells. By contrast, a non-silencing sequence did not alter CDC25A or MT3-MMP levels. Actin blots served as a loading control.

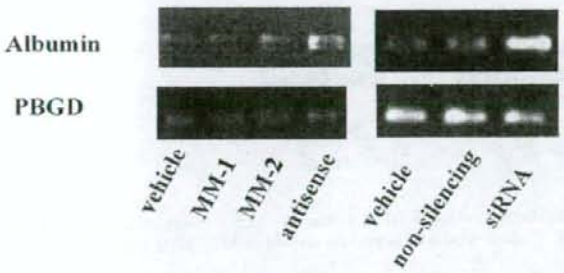

Figure 7. Inhibition of CDC25A induced albumin mRNA expression in PLC cells. AS to CDC25A and siRNA against CDC25A induced expression of albumin mRNA as early as 12 h after treatment. PBGD served as the control.

HCC by restraining growth, which may lead to prolonged disease-free survival.

We also found that AS to CDC25A inhibited the invasive activity of HCC cell lines. This finding is particularly important because HCC invades vessel walls and metastasizes inside the liver, which is considered a major cause of death from the disease (29,30). It may be argued that the inhibitory effects of AS to CDC25A on cancer cell invasion may simply reflect reduced tumor cell growth. We cannot rule out such a possibility. Yet based on the demonstrated downregulation of MT3-MMP in all three HCC cell lines it is likely that the invasive ability itself may be regulated by AS to CDC25A. MT3-MMP, one of the major MMPs, was originally cloned from human melanoma tissue and human placenta and is expressed in a variety of normal and tumor tissues (22,31-33). Functional expression of MT3-MMP in human WM1341D melanoma cells facilitated *in vitro* collagen I invasion (34). Also, expression of MT3-MMP in hamster CHO-K1 and canine MDCK cells induced the expression of a fibrin-invasive phenotype (35). When we examined the mRNA expression of MMP2, MT1-MMP, MT2-MMP, and MT3-MMP in HCC and gastrointestinal cancer cell lines, we found that MT3-MMP expression was rather specific to HCC cell lines. Moreover, we recently found that MT3-MMP expression was associated with tumor invasion in primary HCC tissues (36). Although the precise mechanism of how CDC25A regulates MT3-MMP should be determined at the next stage of research, these findings suggest the relevance of MT3-MMP to invasion in HCC.

Our previous study showed that CDC25A expression was associated with dedifferentiated histology of HCC (14). In the present mechanistic study, we found upregulation of albumin mRNA in PLC cells treated with CDC25A AS. It is reported that PLC produces albumin scarcely, while Huh-7 and HepG2 cells produce high albumin levels (37-39), which is consistent with current findings. The difference in basal albumin level may account for restoration of albumin expression only in PLC cells. Human HCC is unique in that tumor growth occurs relatively slowly and with a well-differentiated phenotype in the early stage but faster and with dedifferentiation in the advanced stage (40,41). In this context, inhibition of CDC25A may convert advanced HCC into a more differentiated and less aggressive phenotype; at least certain types of HCC cells.

In conclusion, antagonism of CDC25A inhibited the growth and invasion of HCC cells, possibly via cell cycle arrest at G0-G1 and suppression of MT3-MMP expression. Taken together, these findings strongly suggest that CDC25A may be a promising therapeutic target against HCC. Indeed, several CDC25A inhibitors are being developed, including novel vitamin K analogues and steroidal-derived inhibitors (42,43).

Acknowledgements

This study was supported by a Grant-in Aid for Cancer Research from the Ministry of Education, Science, Sports, Culture, and Technology, Japan to H.Y.

EUROPEAN JOURNAL OF CANCER 44 (2008) 885–897

available at www.sciencedirect.com

ScienceDirect

journal homepage: www.ejconline.com

Molecular mapping of human hepatocellular carcinoma provides deeper biological insight from genomic data

Nobuyoshi Kittaka[a], Ichiro Takemasa[a,], Yutaka Takeda[a], Shigeru Marubashi[a], Hiroaki Nagano[a], Koji Umeshita[a], Keizo Dono[a], Kenichi Matsubara[b], Nariaki Matsuura[c], Morito Monden[a]*

[a]*Department of Surgery, Graduate School of Medicine, Osaka University, 2-2 Yamadaoka E-2, Suita, Osaka 565-0871, Japan*
[b]*DNA Chip Research Inc., 1-1-43 Suehirocho, Tsurumi-ku, Yokohama 230-0045, Japan*
[c]*Department of Functional Diagnostic Science, Osaka University Graduate School of Medicine, 1-7 Yamadaoka, Suita, Osaka 565-0871, Japan*

ARTICLE INFO

Article history:
Received 5 December 2007
Received in revised form
5 February 2008
Accepted 12 February 2008
Available online 11 March 2008

Keywords:
DNA microarray
Network analysis
Integrative method
'Hotspot' region
Biological insight

ABSTRACT

DNA microarray analysis of human cancer has resulted in considerable accumulation of global gene profiles. However, extraction and understanding the underlying biology of cancer progression remains a significant challenge. This study applied a novel integrative computational and analytical approach to this challenge in human hepatocellular carcinoma (HCC) with the aim of identifying potential molecular markers or novel therapeutic targets. We analysed 100 HCC tissue samples by human 30 K DNA microarray. The gene expression data were uploaded into the network analysis tool, and the biological networks were displayed graphically. We identified several activated 'hotspot' regions harbouring a concentration of upregulated genes. Several 'hotspot' regions revealed integrin and Akt/NF-κB signalling. We identified key members linked to these signalling pathways including osteopontin (SPP1), glypican-3 (GPC3), annexin 2 (ANXA2), S100A10 and vimentin (VIM). Our integrative approach should significantly enhance the power of microarray data in identifying novel potential targets in human cancer.

© 2008 Elsevier Ltd. All rights reserved.

1. Introduction

Investigation of various cancers at the molecular level is well underway through functional approaches including DNA microarray technology that can simultaneously detect the expression levels of tens of thousands of genes. The resulting wealth of data has been analysed with a variety of clustering, partitioning and pattern-matching algorithms in the quest to generate molecular signatures for several human malignant tumours with respect to their stage, prognostic outcome and response to therapy.

Notwithstanding the obvious power of the genomic data generated, these molecular analyses have not yielded the expected advances in our understanding of the mechanisms of cancer development, or the identification of critical genomic and molecular aberrations that would improve the precision of diagnosis or serve as therapeutic targets. This is mainly due to the overwhelming diversity of genome-wide interactions and gene-expression patterns, which limit effective learning from experimental data alone. Network analysis technologies are currently addressing this problem by mapping the gene expression data into relevant networks based on known mammalian biology, derived from basic and clinical research. To this end, our group has combined microarray analysis with a computational tool to obtain further biological insights into the regulatory networks of differentially expressed genes and

* *Corresponding author:* Tel.: +81 6 6879 3251; fax: +81 6 6879 3259.
E-mail address: alfa-t@sf6.so-net.ne.jp (I. Takemasa).
0959-8049/$ - see front matter © 2008 Elsevier Ltd. All rights reserved.
doi:10.1016/j.ejca.2008.02.019

the corresponding canonical pathways related to the progression of cancer. We applied this integrative approach to human hepatocellular carcinoma (HCC), the fifth most common malignancy worldwide.[1,2] Despite the remarkable improvements in diagnosis and patient management, the outcome for patients with HCC remains grave, mainly due to the advanced tumour stage accelerated by intrahepatic tumour spread and frequent tumour recurrence.[3] Hepatocarcinogenesis is a multistep process involving somatic mutations, loss of tumour suppressor genes and possibly the activation or overexpression of certain oncogenes.[4] These events lead to changes in the expression of numerous genes, and comparison of gene expression patterns between HCC and normal liver tissue is a popular method for characterising tumour properties and identifying novel target genes for possible therapy. However, this method has not proven to be sufficiently definitive in identifying genetic determinants of specific HCC regulatory pathways. New approaches are urgently needed to better understand the underlying mechanisms of hepatocarcinogenesis, and to develop new therapeutic approaches targeted to HCC-specific molecular abnormalities. By highlighting several activated regions in the genome (known as 'hotspot' regions[5,6]) involved in regulating the progression of HCC, we have identified significantly upregulated genes linked to these 'hotspot' pathways as potential key molecules.

Our integrative analysis revealed two 'hotspot' canonical pathways (integrin and Akt/NF-κB signalling pathways) and identified five potential key genes that were upregulated in the majority of HCC tumours. We further investigated two of these potential key molecules, ANXA2 and S100A10, which were upregulated at the protein and mRNA levels in most HCC samples. Importantly, because it is proteins that function in networks controlling critical cellular events,[7] it is reasonable to speculate that coexpression of ANXA2 and S100A10 at the protein level might have an impact on hepatocarcinogenesis through the activated 'hotspot' pathway.

2. Materials and methods

2.1. Tissue samples

Samples from 100 HCC tissues and seven normal livers without virus infection were obtained with informed consent from patients who underwent hepatic resection at Osaka University Hospital from 1997 to 2003. Tissue specimens (approximately 5 mm^3) for RNA isolation were stored at −80 °C until use. All tissue specimens were submitted for routine pathological evaluation and confirmation of diagnosis. The histopathological characterisation of HCC was based on the Classification of the Liver Cancer Study Group of Japan. Table 1 lists the clinicopathological features of the 100 cases of HCC.

2.2. Extraction and quality assessment of RNA

Total RNA was purified from tissue samples using TRIzol reagent (Invitrogen, San Diego, CA) as described by the manufacturer. The integrity of RNA was assessed on an Agilent 2100 Bioanalyzer and RNA 6000 LabChip kits (Yokokawa Ana-

Table 1 – Clinicopathological characteristics of 100 patients with HCC

Clinicopathological features	n
Age	
Median	66
Range	47–81
Gender	
Male	81
Female	19
Virus	
HBV	21
HCV	40
Both	28
None	11
Child-Turcotte-Pugh stage	
A	77
B	23
C	0
Liver cirrhosis	
Present	42
Absent	58
AFP	
<200 ng/ml	71
⩾200 ng/mg	29
PIVKA-II	
<50mAU/ml	36
⩾50mAU/ml	64
Tumour size	
<5.0 cm	76
⩾5.0 cm	24
Edmonson grading	
1–2	43
3–4	57
Histologic type of tumour	
Well differentiated	4
Moderately differentiated	41
Poorly differentiated	55
Vascular invasion	
Present	41
Absent	59
Intrahepatic metastasis	
Present	22
Absent	78
Pathological stage	
I	23
II	52
III	20
IVA	5
CLIP score	
0	56
1	35
2	8
3	0
4	1
5	0
6	0
JIS score	
0	18
1	46
2	26
3	9
4	1
5	0

CLIP score; The cancer of Liver Italian Program score.
JIS score; The Japan Integrated Staging score.

lytical Systems, Tokyo, Japan). Only high-quality RNA with intact 18s and 28s RNA was used for subsequent analysis. Seven RNA extractions from different normal liver tissue were mixed as the control reference.

2.3. *Preparation of fluorescently labelled aRNA targets and hybridisation*

Extracted RNA samples were amplified with T7 RNA polymerase using the Amino Allyl MessageAmp™ aRNA kit (Ambion, Austin, TM) according to the protocol provided by the manufacturer. The quality of each Amino Allyl-aRNA sample was checked on the Agilent 2100 Bioanalyzer. Five micrograms of control and experimental aRNA samples were labelled with Cy3 and Cy5, respectively, mixed and hybridised on an oligonucleotide microarray covering 30,336 human probes (AceGene Human 30K; DNA Chip Research Inc. and Hitachi Software Engineering Co., Yokohama, Japan). The experimental protocol is available at http://www.dna-chip.co.jp/thesis/AceGeneProtocol.pdf. The microarrays were scanned on a ScanArray 4000 (GSI Lumonics, Billerica, MA).

2.4. *Analysis of microarray data*

Signal values were calculated using DNASIS Array Software (Hitachi Software Inc., Tokyo). Following background subtraction, data with low signal intensities were excluded from additional investigation. In each sample, the Cy5/Cy3 ratio values were log-transformed. Then, global equalisation to remove a deviation of the signal intensity between whole Cy3- and Cy5-fluorescence was performed by subtracting the median of all log(Cy5/Cy3) values from each log(Cy5/Cy3) value. Genes with missing values in more than 20% of samples were excluded from further analysis; a total of 16,923 genes out of 30,336 were available for analysis.

2.5. *Gene network analysis*

We further analysed the signature genes of HCC by Ingenuity Pathways Analysis (Ingenuity systems, Mountain View, CA; http://www.ingenuity.com), a web-delivered application that enables biologists to discover, visualise and explore relevant networks significant to their experimental results, such as gene expression array datasets. The application makes use of the Ingenuity Pathways Knowledge Base (IPKB), which contains large amounts of individually modelled relationships between gene objects (e.g., genes, mRNAs and proteins) to dynamically generate significant biological networks and pathways. The submitted genes that are mapped to the corresponding gene objects in the IPKB are called 'focus genes'. The focus genes are used as the starting point for generating biological networks. To start building a network, the Ingenuity software queries the IPKB for interactions between focus genes and all the other genes stored in the IPKB, and then generates a set of networks with a maximum network size of 35 genes. A p value for each network is calculated according to the fit of the user's set of significant genes. This is accomplished by comparing the number of focus genes that participate in a given network relative to the total number of occurrences of those genes in all networks stored in the IPKB. The score of a network is displayed as the negative log of the p value, indicating the probability that a collection of genes equal to or greater than the number in a network could be achieved by chance alone.

2.6. *Selection of candidate genes expressed in HCC*

To identify molecular pathways that may be activated or suppressed in HCC, we used a network knowledge-base approach, Ingenuity Pathway Analysis Software, to analyse genome-wide transcriptional responses in the context of known functional interrelationships amongst proteins, small molecules and phenotypes. The post-normalised genes (16,923 genes) either up- or down-regulated in the microarray data, were uploaded into the IPKB as a tab-delimited text file of GenBank accession numbers. These biological networks comprising 5936 genes are displayed graphically as nodes (genes/gene products) and edges (the biological relationships between the nodes). The nodes are displayed using various shapes that represent the functional class of the gene product. The colour green reflects downregulation of gene expression, and red represents upregulation of gene expression with the significance of that regulation represented by colour intensity. Edges are displayed with various labels that describe the nature of the relationship between the nodes. In this way, simultaneous survey and evaluation of the subnetwork regions enabled us to identify several activated canonical pathways in HCC. We highlighted new molecules linked to the 'hotspot' canonical pathways.

2.7. *Real-time quantitative RT-PCR analysis*

Total RNA (1 μg) was used for reverse transcription, and complementary DNA (cDNA) was generated using the Reverse Transcription System (Promega, Madison, WI) as described previously.[8] Quantification of mRNA expression of the candidate genes listed in Table 2 was performed using a real-time thermal cycler, the LightCycler and detection system (Roche Diagnostics, Mannheim, Germany). For detection of the amplification products, LightCycler-DNA master SYBR green I (Boehringer

Table 2 – Candidate genes and expression ratio of microarray analysis

CDS ID	Gene symbol	Description	Average of Cy5/Cy3
NM_000582	SPP1	Secreted phosphoprotein 1 (osteopontin)	4.69
NM_004484	GPC3	Glypican 3	4.23
NM_004039	ANXA2	Annexin 2	2.86
M38591	S100A10	Cellular ligand of annexin 2	1.97
NM_003380	VIM	Vimentin	1.82

Mannheim, Mannheim, Germany) was used as described previously.[9] Briefly, a 20 μl reaction volume containing 2 μl of cDNA and 0.2 μmol/l of each primer was applied to a glass capillary. The primer sequences, PCR cycle conditions and annealing temperatures are listed in Supplementary Table 1. Quantitative analysis of mRNA was performed using LightCycler analysis software (Roche Diagnostics). The relative expression level of the candidate gene was computed with respect to the internal standard GAPDH mRNA to normalise for variations in the amount of input cDNA. The level of expression of the candidate gene was provided by the ratio, in which each normalised gene value in tissue samples was divided by GAPDH mRNA in the same control reference used in the microarray assay. We compared the ratio of candidate genes between samples randomly selected out of 100 HCC samples.

2.8. Immunohistochemical staining

Formalin-fixed, paraffin-embedded samples were cut into 5 μm sections, and these were deparaffinised in xylene and rehydrated through a graded series of ethanol. Immunohistochemical staining was performed using a Vectastain ABC peroxidase kit (Vector Labs, Burlingame, CA) as described previously.[10] Briefly, the sections were treated for antigen retrieval in 0.01 M sodium citrate buffer (pH 6.0) for 40 min at 95 °C, followed by incubation in methanol containing 0.3% hydrogen peroxide at room temperature for 20 min to block endogenous peroxidase. After blocking endogenous biotin, the sections were incubated with normal protein-block serum solution at room temperature for 20 min, to block non-specific staining, and then incubated overnight at 4 °C with anti-ANXA2 (mouse monoclonal IgG, diluted 1:500, Abcam Inc.), anti-S100A10 (mouse monoclonal IgG, diluted 1:400, Swant Inc.) and anti-GPC3 (mouse monoclonal IgG, University of Toronto, Jorge Filmus et al.[11]) as primary antibodies. After washing three times for 5 min in phosphate buffered saline (PBS), sections were incubated with a biotin-conjugated secondary antibody (horse anti-mouse for ANXA2, S100A10 and GPC3) at room temperature for 20 min and finally incubated with peroxidase-conjugated streptavidin at room temperature for 20 min. The peroxidase reaction was then developed with 3,3′-diaminobenzidine tetrachloride (Wako Pure Chemical Industries, Osaka, Japan). Finally, the sections were counterstained with Mayer's haematoxylin. For negative controls, sections were treated the same way except they were incubated with non-immunised rabbit IgG or Tris-buffered saline instead of the primary antibody. Immunohistochemical staining was assessed by two investigators independently, without the knowledge of the corresponding clinicopathological data.

2.9. Statistical analysis

Pearson's correlation coefficient, χ^2 test, *t*-test and Kaplan–Meier plot were analysed using StatView (Version 5.0) software (Abacus Concepts, Berkeley, CA). *p* values less than 0.05 were considered statistically significant. Hierarchical cluster analysis (HCA) was performed with Euclidean distance coefficient as a similarity coefficient and the unweighted pair group method using arithmetic averages (UPGMA) as the clustering algorithm, using GeneMaths (Version 2.0) software.

3. Results

3.1. Microarray analysis of gene expression changes in HCC tumours

Gene expression profiling of primary HCC tumours from 100 patients was examined by DNA microarray. We calculated the mean expression levels of each gene across all HCC samples, and, as a preliminary analysis, identified the top 2% of candidate genes displaying at least a 1.5-fold increase in expression. These highly upregulated genes included α-fetoprotein (AFP; data not shown), a common prognostic marker for HCC (fold change = 1.56), and GPC3, recently identified as a novel tumour marker of HCC (fold change = 4.23; fourth highest upregulation).

3.2. Identification of biologically relevant networks and potential key genes highly expressed in HCC tumours

In our global network comprising 5936 genes (Supplementary Fig. 1), we highlighted integrin and Akt/NF-κB signalling as two 'hotspot' pathways that comprised a concentration of upregulated genes. The integrin signalling pathway shown in Fig. 1A (gene subnetworks listed in Supplementary Table 2) was identified as significantly activated in HCC and contained 11 upregulated genes, flagging this pathway as a key regulator in HCC tumourigenesis. This fits with the role of integrin signalling in promoting cell proliferation and cell motility.[12] Furthermore, SPP1 and GPC3 were identified as potential key genes (upregulated with >1.5-fold change), with links to integrin signalling. Similarly, we identified the activation of the Akt/NF-κB pathway shown in Fig. 1B in HCC tumours (gene subnetworks listed in Supplementary Table 3). This signalling pathway contained 12 upregulated genes and plays key roles in many cell processes relevant to tumourigenesis including cell survival and apoptosis.[13] Amongst the genes linked to Akt/NF-κB signalling and that had >1.5-fold change were ANXA2, S100A10 and VIM. Network analysis revealed a link between Akt/NF-κB signalling and both ANXA2 and S100A10 through interactions with β-actin (ACTB) and E-cadherin (CDH1). These candidate genes are listed in Table 2.

3.3. Quantitative RT-PCR validation of several selected genes

To validate the microarray data, we performed quantitative RT-PCR for candidate genes in 20 samples randomly selected out of the 100 HCC tissues. We compared gene expression levels generated from quantitative RT-PCR with those from microarray analysis by Pearson's correlation coefficients for each candidate gene and StatView Software (Fig. 2). Each of the five genes analysed showed significant correlation confirming the results obtained by DNA microarray.

3.4. Immunohistochemical study of glypican 3, Annexin 2 and S100A10 in patient samples

Of the five genes overexpressed in HCC tumours by RT-PCR, immunohistochemical staining for GPC3 was performed on 10 samples of HCC and surrounding non-cancerous tissues

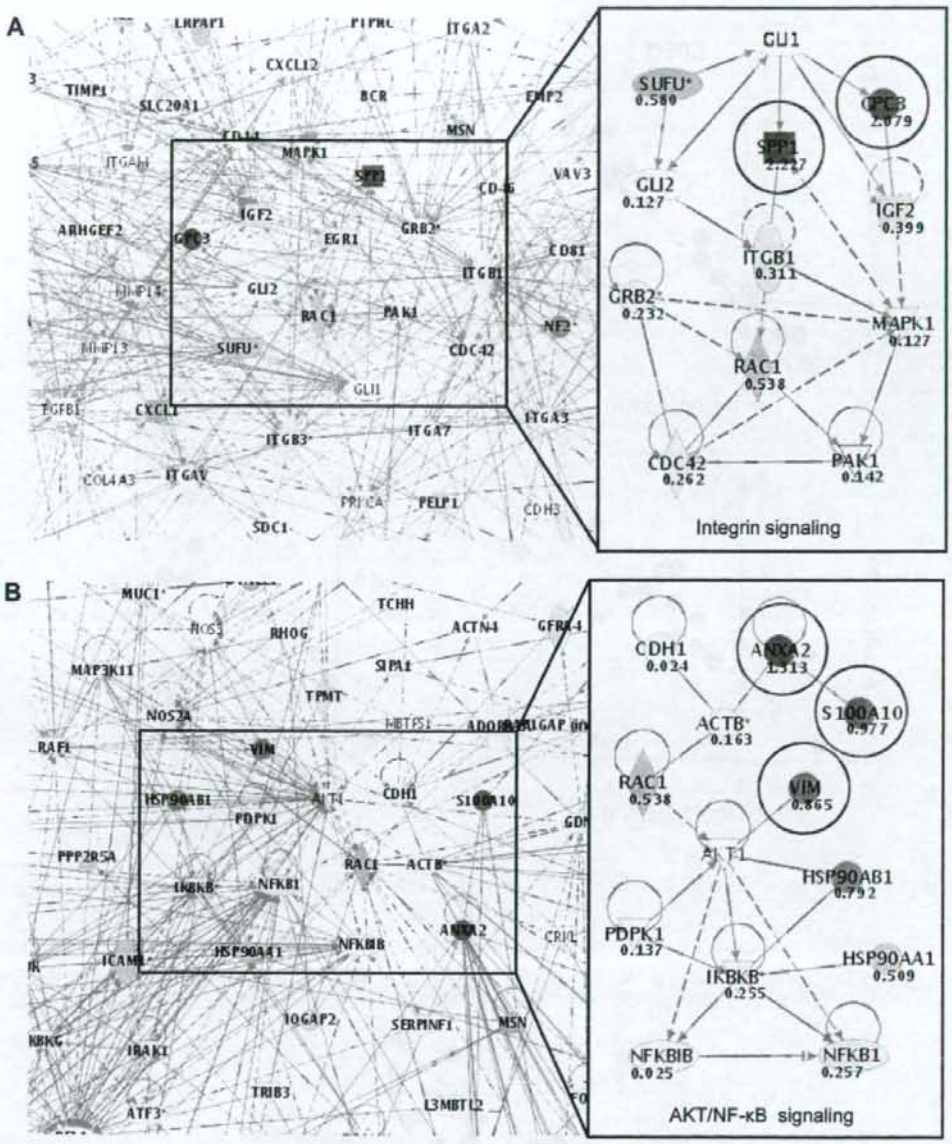

Fig. 1 – (A) The integrated method of DNA microarray and Ingenuity Pathway Analysis produced a network with 'hotspot' regions harbouring concentrations of upregulated genes. These genes included ITGB1 (integrin, beta 1), RAC1 (ras-related C3 botulinum toxin substrate 1), GRB2 (growth factor receptor-bound protein 2), CDC42 (cell division cycle 42), PAK1 (p21/Cdc42/Rac1-activated kinase 1) and MAPK1, which are all associated with integrin signalling. SPP1, GPC3, GLI1, GLI2, SUFU (suppressor of fused homolog) and IGF2 are also linked to this pathway. The circled genes, SPP1 and GPC3, were selected as candidate genes. The numerical value of each gene represents the median of all log(Cy5/Cy3) values. (B) The integrative method showed a second network including a 'hotspot' region. This region contained AKT1 (v-akt murine thymoma viral oncogene homolog 1), PDPK1 (3-phosphoinositide-dependent protein kinase-1), NFKBIB (nuclear factor of kappa light polypeptide gene enhancer in B-cells inhibitor, beta), NFKB1 (nuclear factor of kappa light polypeptide gene enhancer in B-cells 1), IKBKB (inhibitor of kappa light polypeptide gene enhancer in B-cells, kinase beta), HSP90AA1 (heat shock protein 90 kDa alpha, class A member 1) and HSP90AB1 (heat shock protein 90 kDa alpha, class B member 1), which are all associated with the Akt/NF-κB signalling pathway. ANXA2, S100A10, ACTB, CDH1 and VIM are also linked to this pathway. The circled genes, ANXA2, S100A10 and VIM, were selected as candidate genes. The numerical value of each gene represents the average of all log(Cy5/Cy3) values.

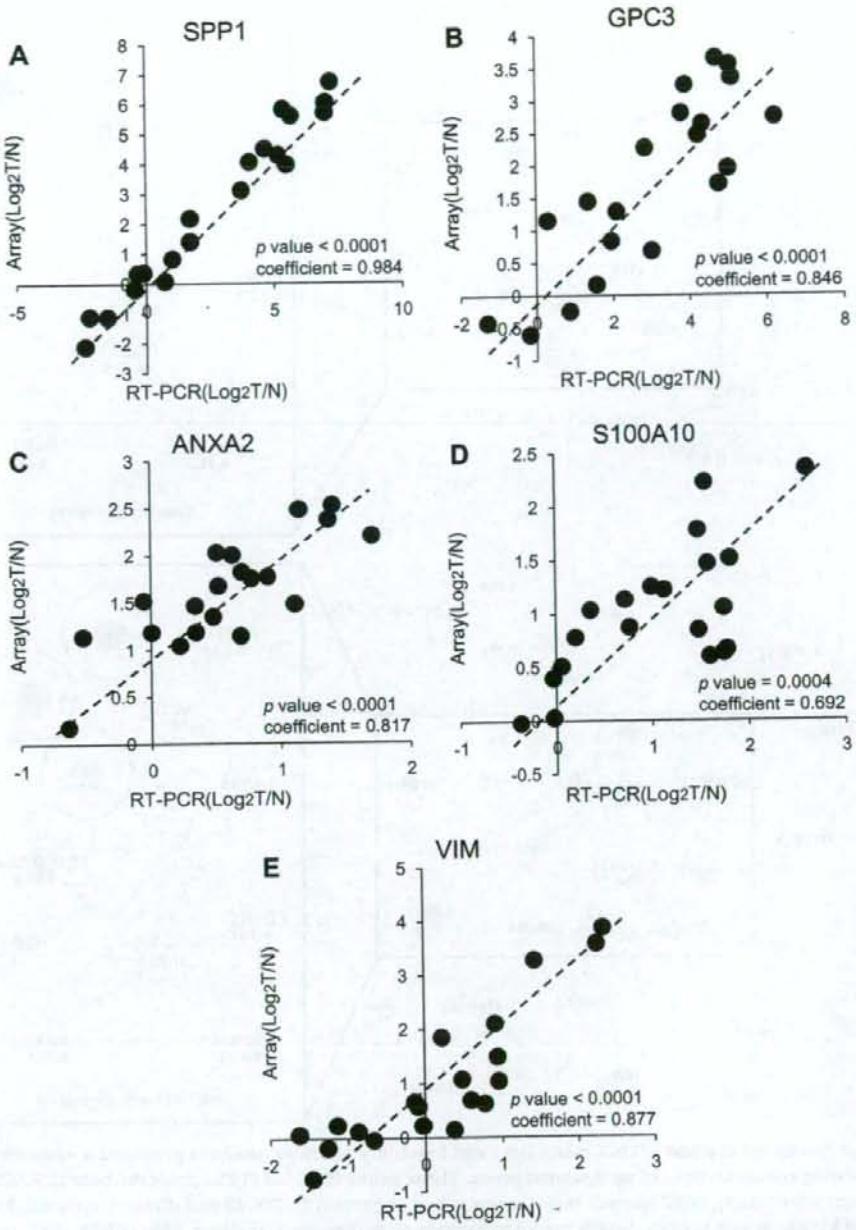

Fig. 2 – Results of quantitative RT-PCR on 20 samples randomly selected from the 100 HCC samples. Individual mRNA levels were normalised to GAPDH and expressed relative to those in a mixture of seven normal livers for SPP1, GPC3, ANXA2, S100A10 and VIM. We compared gene expression levels generated from quantitative RT-PCR with those from microarray analysis and used Pearson's correlation analysis for each candidate gene using StatView Software. (A), (B), (C), (D) and (E) show the correlation of SPP1, GPC3, ANXA2, S100A10 and VIM, respectively.

(Fig. 3A and B). GPC3 expression was observed in 7 of 10 cases of moderately or poorly differentiated HCC. As published previously,[11] staining of GPC3 was observed in a coarsely granular pattern near the cell membrane (2/7) and dispersed evenly in the cytoplasm (5/7). GPC3 expression was undetectable in all non-neoplastic tissues with diffuse hepatitis changes.

Immunohistochemical staining of ANXA2 and S100A10 was then performed on 20 paraffin-embedded samples of HCC and surrounding non-cancerous tissues. The Ca^{2+}-

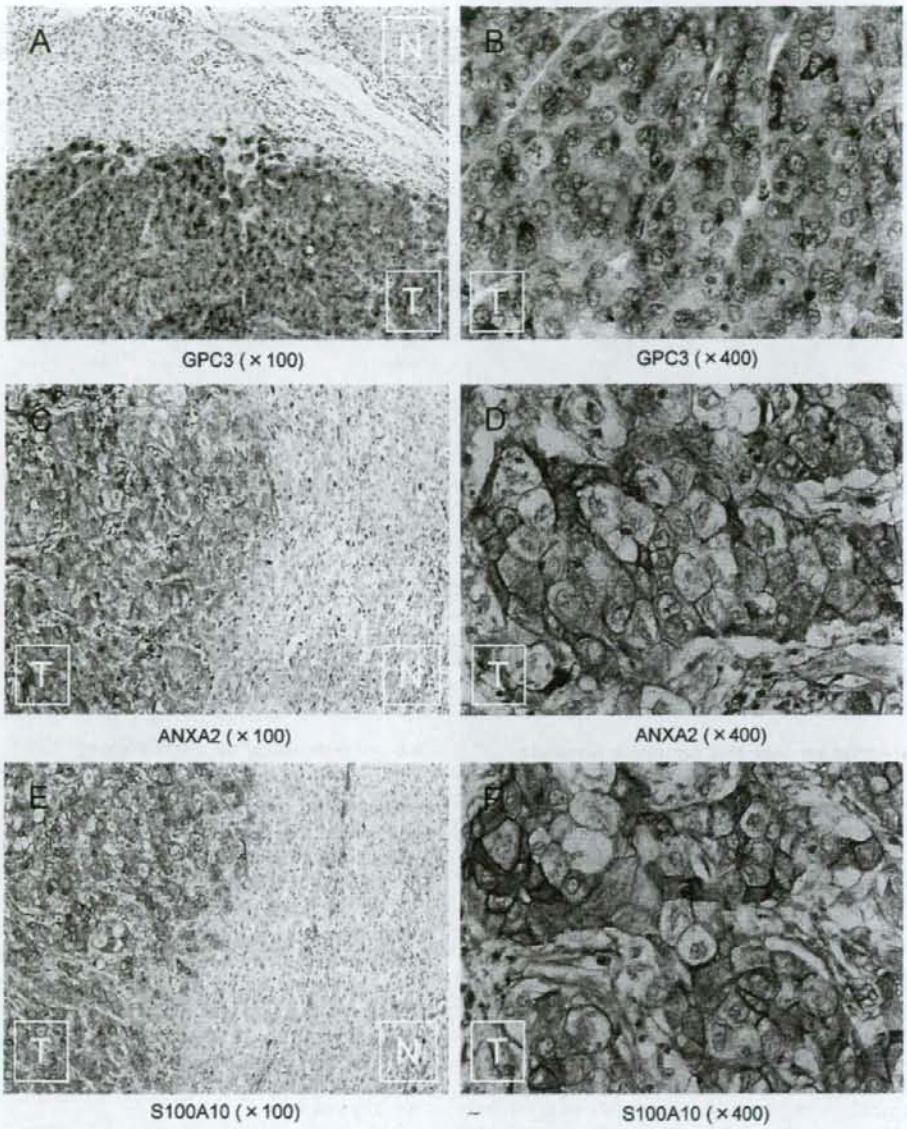

Fig. 3 – (A and B) GPC3 protein expression in human HCC tissue. Brown GPC3 immunostaining is evident in cancer cells. Note the diffuse non-granular staining pattern in the cytoplasm. (C and D) ANXA2 protein expression in human HCC tissue. Note ANXA2 staining in the cell membrane of cancer cells, with slight immunoreactivity in the cytoplasm. (E and F) S100A10 protein expression in human HCC tissues. Note S100A10 staining at the cell membrane of cancer cells. C, D, E and F are from the same tissue sample, and staining for S100A10 overlapped significant with ANXA2 staining. (A, C and E) ×100 magnification. (B, D and F) ×400 magnification. T; tumour region. N; normal liver.

and membrane-binding protein ANXA2 can form a hetero-tetrameric complex with S100A10 and this complex is thought to serve as a bridging or scaffolding function in the membrane underlying cytoskeleton.[14] Previous studies demonstrated both ANXA2 and S100A10 at the plasma membrane in hepatoblastoma HepG2 cell lines,[15] but not in human HCC tissues. Immunohistochemical staining of ANXA2 and S100A10 was stronger at the plasma membrane of the same samples than in the cytoplasm (Fig. 3C–F). The immunoreactivity for ANXA2 was heterogeneous, and cancerous tissues were immunopositive in 16 samples. Endothelial cells were immunopositive for ANXA2 in all samples tested. Similarly, staining of S100A10 was heterogeneous, and cancerous tissues were immunopositive in 17 samples.

Table 3 – Clinicopathological characteristics and results of immunohistochemical staining of ANXA2 and S100A10

Patient	Age	Gender	Hepatitis virus infection	Histological type	Vascular invasion	Annexin2 expression	S100A10 expression
Case 1	71	M	HCV	por	–	++	++
Case 2	66	F	HBV	mod	+	++	++
Case 3	38	M	HBV	mod	+	++	++
Case 4	65	M	HCV	por	+	++	++
Case 5	59	M	HCV	por	–	++	++
Case 6	72	F	HCV	mod	–	+	++
Case 7	71	M	–	por	–	++	+
Case 8	72	M	HBV, HCV	por	–	++	+
Case 9	61	M	–	por	–	++	+
Case 10	78	M	HCV	por	–	++	+
Case 11	49	F	HBV	por	+	++	+
Case 12	72	F	HBV	por	+	+	+
Case 13	68	M	HBV, HCV	mod	–	+	+
Case 14	78	F	HBV, HCV	mod	–	+	+
Case 15	74	M	HBV, HCV	well	–	+	+
Case 16	67	M	–	mod	–	–	+
Case 17	53	M	HBV	mod	+	–	–
Case 18	75	M	HCV	por	–	–	–
Case 19	66	M	HBV, HCV	mod	+	–	–
Case 20	60	M	HCV	por	–	–	–

++, strong immunopositive; +, partial immunopositive; –, immunonegative.

Colocalisation of ANXA2 and S100A10 was observed in 15 samples (Table 3).

3.5. *Correlation between gene expression signature of the two 'hotspot' and clinicopathological features*

Next, to better understand if any of the two 'hotspot' identified by this integrated approach correlates with clinicopathological features, a hierarchical clustering of all 100 HCC samples using the upregulated genes included in the 'hotspot' was performed. Fig. 4A shows the gene expression profiles using the 11 genes upregulated in the 'hotspot 1 (integrin signalling)'. Examination of this result allowed identification of three subgroups; 'relatively high-activated group ($n = 39$), defined as Group A1', 'intermediate-activated group ($n = 45$), defined as Group A2', and 'relatively low-activated group ($n = 16$), defined as Group A3'. Likewise, Fig. 4B shows the gene expression profiles using the 12 genes upregulated in the 'hotspot 2 (Akt/NF-κB signalling)'. Examination of this result also identified two subgroups; 'relatively high-activated group ($n = 17$), defined as Group B1' and 'relatively low-activated group ($n = 83$), defined as Group B2'. Having identified the two distinctive subgroups; 'relatively high-activated group' and 'relatively low-activated group' in each of the two 'hotspots', we examined the association between the activation of 'hotspot' and clinicopathological data (Table 4A and B). In the integrin signalling, the activated profile was significantly associated with intrahepatic metastasis ($p = 0.012$), tumour size ($p = 0.023$) and Edmonson grading ($p < 0.001$). On the other hand, in the Akt/NF-κB signalling, the activated profile was significantly associated with Edmonson grading ($p = 0.004$). Kaplan–Meier plot showed a significant difference in the probability of disease-free survival ($p = 0.037$) and overall survival ($p = 0.045$) between 'Group A1' and 'Group A3' in the integrin signalling (Fig. 4C and D). In the Akt/NF-κB signalling, a significant difference was observed in disease-free survival ($p = 0.045$, Fig. 4E and F).

3.6. *Overview of the distribution of differentially expressed genes on human chromosome*

To compare our microarray data with chromosomal aberrations in HCC, we also investigated the chromosomal region in which the differentially expressed genes were harboured. The public source for annotating the location of each gene was the National Center for Biotechnology Information (NCBI). This investigation revealed that the regions of high density of 100 upregulated genes tended to be at chromosomes 1q, 6p and 8q (Fig. 5A), whilst those of 100 downregulated genes were at chromosomes 4q and 16q (Fig. 5B). Furthermore, SPP1, GPC3, ANXA2 and S100A10, identified as key molecules, were separately located at chromosomes 4q, Xq, 15q and 1q.

4. Discussion

In the post-genomic period, DNA microarray technology is used to monitor disease progress and to individualise treatment regimens. However, extracting new biological insights from high-throughput genomic studies of cancer progression poses a challenge due to difficulties in recognising and evaluating relevant biological processes from vast quantities of experimental data. Although other high-throughput technologies in protein expression (proteomics) and low-molecular weight metabolite expression (metabolomics) have made remarkable progress, no comprehensive analytical techniques exist that can measure more than 500,000 protein forms and 100,000–1,000,000 metabolites quantitatively.[16] Generating biological networks from comprehensive gene expression profiles manually in a visual manner could be used to navigate

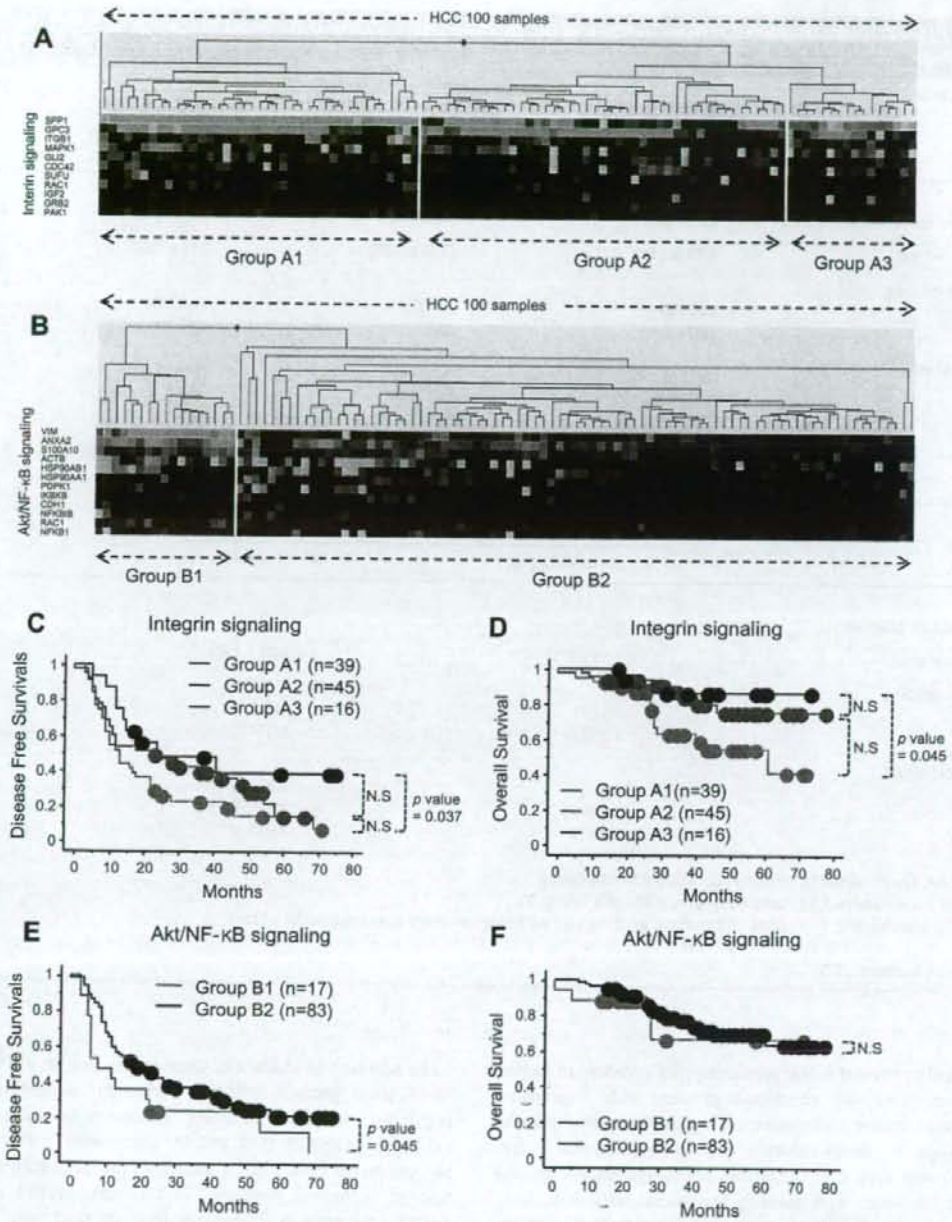

Fig. 4 – (A) Hierarchical clustering analysis of all 100 HCC samples using the 11 upregulated genes included in the 'hotspot 1 (integrin signalling)'. Red and green indicate relative high- and low-expression, respectively. Based on the similarities of their gene expression profiles, samples were grouped in 'relatively high-activated group ($n = 39$), defined as Group A1', 'intermediate-activated group ($n = 45$), defined as Group A2', and 'relatively low-activated group ($n = 16$), defined as Group A3'. (B) A hierarchical clustering analysis of all 100 HCC samples using the 12 upregulated genes included in the 'hotspot 2 (Akt/NF-κB signalling)'. Based on the similarities of their gene expression profiles, samples were grouped in 'relatively high-activated group ($n = 17$), defined as Group B1' and 'relatively low-activated group ($n = 83$), defined as Group B2'. (C and D) Disease-free survival and overall survival of each of the activated groups in the 'hotspot 1 (integrin signalling)' (Kaplan–Meier plot). The log-rank p value is shown. NS, not significant. (E and F) Disease-free survival and overall survival of each of the activated groups in the 'hotspot 2 (Akt/NF-κB signalling)' (Kaplan–Meier plot). The log-rank p value is shown. NS, not significant.

Table 4 – Clinical and pathological characteristics of the high-activated and low-activated groups in each of integrin signalling and AKT/NF-κB signalling

Characteristics	Integrin signalling ('Hotspot' 1)			p value
	Group A1 ($n = 39$)	Group A2 ($n = 45$)	Group A3 ($n = 16$)	
	No. of patients (%)	No. of patients (%)	No. of patients(%)	
A				
Intrahepatic metastasis	12(30.8)	(10(22.2))	0(0)	0.012
Tumour size (cm)	4.79 ± 3.12	(3.49 ± 1.75)	2.91 ± 1.22	0.023
Edmonson grading				
1–2	11(28.2)	22(48.9)	10(62.5)	<0.001
3–4	28(71.8)	23(51.1)	6(37.5)	
Pathological stage				
I	5(12.8)	15(33.3)	3(18.7)	0.642
II	22(56.4)	20(44.4)	10(62.5)	
III	9(23.1)	8(17.8)	3(18.7)	
IVA	3(7.7)	2(4.5)	0	

Characteristics	Akt/NF-κB signalling ('Hotspot' 2)		p value
	Group B1 ($n = 17$)	Group B2 ($n = 83$)	
	No. of patients (%)	No. of patients (%)	
B			
Intrahepatic metastasis	4(23.5)	18(21.7)	0.867
Tumour size (cm)	4.55 ± 2.58	3.88 ± 2.81	0.226
Edmonson grading			
1–2	2(11.7)	41(49.4)	0.004
3–4	15(88.3)	42(50.6)	
Pathological stage			
I	1(5.9)	22(26.5)	0.333
II	11(64.7)	41(49.4)	
III	4(23.5)	16(19.3)	
IVA	1(5.9)	4(4.8)	

p values of A are obtained by comparing Group A1 with Group A3.
p values of B are obtained by comparing Group B1 with Group B2.
p values for intrahepatic metastasis, Edmonson grading and pathological stage are obtained by χ^2 test.
p value for tumour size is obtained by t test.
Tumour size is mean ± SD.

through and unravel the complex networks involved in cancer progression. Here, we combined genome-wide expression analysis with a new bioinformatics method, Ingenuity Pathway Analysis, to clarify the relationship between the microarray datasets and the canonical pathways based on the published literature and identify functional networks, 'hotspot', responsible for the progression of HCC. Furthermore, we discovered several molecules commonly upregulated in HCC as potential key players in the neoplastic process.

This combined approach revealed that several distinct regions with upregulated genes were concentrated. These concentrations of activated genes included several genes involved in the WNT signalling pathway, which has been the subject of intense research in recent years. In addition, we highlighted integrin and Akt/NF-κB as two 'hotspot' signalling pathways, and propose that these signalling pathways are crucial for the core biological functions in HCC progression and potential intervention, such as cell proliferation, cell survival and apoptosis.[17]

In addition to studies of gene expression at the transcriptional level, protein analysis is vital for understanding the regulatory processes in living organisms, because emerging evidence suggests that mRNA expression patterns themselves are necessary but insufficient for quantitative description of biological systems. So far, comparative studies of mRNA and protein abundance indicate that only 20–28% of the total variation of protein abundance can be attributed to mRNA abundance alone.[18] The limiting factors were explained partly by translational processes (microRNAs repress the translation of mRNAs into proteins) and post-translational modification (such as phosphorylation, methylation, acetylation, glycosylation and ubiquitination). In fact, this was the basis for investigating the expression levels of proteins encoded by highly upregulated genes related to key signalling pathways in hepatocarcinogenesis.

Using our analysis protocol, integrin pathway-associated molecules, SPP1 and GPC3, were first identified as key for cell proliferation in HCC. HCC generally spreads throughout the